Ruling Out Chaos in Compact Binary Systems

J. D. Schnittman* and F. A. Rasio†

Department of Physics, Massachusetts Institute of Technology, Cambridge, Massachusetts 02139

We investigate the orbits of compact binary systems during the final inspiral stage before coalescence by integrating the post-Newtonian equations of motion. We include spin-orbit and spin-spin coupling, which, according to a recent study [J. Levin, Phys. Rev. Lett. **84**, 3515 (2000)], may cause the orbits to appear chaotic. To examine this claim, we calculate the divergence of nearby trajectories and attempt to measure the Lyapunov exponent γ. For all systems considered, we find *no chaotic behavior,* placing a lower limit on the divergence time $t_L \equiv 1/\gamma$ that is many times greater than the typical inspiral time, suggesting that chaos should not adversely affect the detection of inspiral events.

For the current generation of ground-based gravitational-wave (GW) detectors, such as LIGO, one of the most promising sources is the final inspiral of two compact stars (black holes or neutron stars in a relativistic binary orbit) [1,2]. To detect such an event successfully, one must be able to match theoretical GW templates to experimental data containing a great deal of instrumental noise. This "matched filtering" technique has the potential of greatly increasing the effective signal-to-noise ratio for the detector [1,3]. Even to specify quantitative *upper limits* on inspiral events (a major objective of early LIGO runs), it is critical to have strong confidence in the physical accuracy of the templates [4].

Recent work has suggested that the orbits of two rapidly spinning compact objects may be chaotic [5,6]. The presence of chaos on the inspiral time scale (typically ~100 s as the frequency sweeps up from ~10 to 10^3 Hz) could significantly reduce the probability of detection, even with GW templates that include spin effects [7]. In the matched filtering technique, if the signal and template are off by as little as half a wavelength (over $\sim10^3$ cycles), the event could be missed because of destructive interference [3]. In order to quantify this threat, we attempt to measure Lyapunov divergence times for a broad sample of initial conditions.

As in the Newtonian two-body problem, a relativistic binary system can be expressed in terms of a reduced mass $\mu = m_1 m_2/(m_1 + m_2)$ orbiting a fixed mass $m = m_1 + m_2$ with a separation $\vec{r} = \vec{r}_1 - \vec{r}_2$. We adopt units with $G = c = m = 1$ and use the same notation and post-Newtonian (PN) equations of motion as described by Kidder [8], expanded to second order (2PN) terms in $(v/c)^2$ and Gm/r, and including spin-orbit (SO) and spin-spin (SS) effects as well as the 2.5PN radiation reaction (RR) term. The individual spins precess because of frame-dragging and the Lens-Thirring effect according to $\dot{\vec{S}}_i = \vec{\Omega}_i \times \vec{S}_i$. Here $i = 1, 2$, $\vec{S}_i$ is the spin of the compact object, and $\vec{\Omega}_i$ is a variable axis of precession as defined in Eq. (2.4) of [7]. The magnitude of $\vec{\Omega}_i$ is the instantaneous spin precession frequency. We also define a mass

ratio $\beta \equiv m_2/m_1$, and a spin-orbit misalignment angle θ_i for each object as the angle between the spin vector $\vec{S}_i$ and the Newtonian angular momentum $\vec{L}_N = \mu(\vec{r} \times \dot{\vec{r}})$. The relative position vector $\vec{r}$ evolves according to a second-order ordinary differential equation of the type $\ddot{\vec{r}} = \vec{a}_{PN} + \vec{a}_{SO} + \vec{a}_{SS} + \vec{a}_{RR}$. The full expressions for these terms can be found in Refs. [6] and [7].

We integrate these equations numerically in double precision using a fifth-order Runge-Kutta scheme with an adaptive time step. The robust nature of the Runge-Kutta algorithm makes it particularly attractive for measuring exponential divergence of nearby trajectories. Indeed, since the Runge-Kutta integration can introduce only errors that grow at a polynomial rate, any exponential divergence, if it occurs, will rapidly dominate the evolution and should be easily distinguishable from numerical effects [9]. To quantify chaotic behavior in a dynamical system, the equations of motion must be conservative in the sense that there should be no dissipative terms that could act as attractors in phase space (which would eliminate the possibility of the system being formally chaotic; see [10]). For this reason, when integrating the equations of motion to calculate Lyapunov exponents, the radiation reaction terms are not included. This also allows for the option of very long integrations to test whether the system is formally chaotic (but on a time scale much longer than the actual inspiral time).

Historically, an important tool for identifying chaos in celestial mechanics has been the Poincaré surface of section [11]. By plotting the position in phase space only at certain values of independent coordinate variables, one can reduce a complicated four-dimensional (4D) phase space trajectory to a 2D scatter plot. Conserved quantities such as energy or angular momentum generally are held constant for different initial conditions plotted on a single section. For many systems, some initial conditions behave regularly, producing 1D curves as if there were additional integrals of the motion, while others fill out 2D regions of the section. This spreading away from the invariant curves is evidence for chaotic behavior in the system. However, this method is successful only in reducing the phase space

by one additional dimension, so for systems with [number of degrees of freedom] − [number of integrals of motion] greater than two, the surface of section technique is not very useful for identifying chaos [12]. For higher-dimensional systems, the projection of nonchaotic orbits onto a two-dimensional section in general will not generate confined curves, and thus a spreading of points in this pseudosection is not necessarily an indication of chaos. For the problem of two spinning compact objects, the phase space is 10D (3 from $\vec{r}$, 3 from $\dot{\vec{r}}$, and 2 each from the spin vectors $\vec{S}_1$ and $\vec{S}_2$, which can precess in arbitrary orientations but maintain constant magnitude [13]) while there are only four obvious constraints, corresponding to angular momentum and energy conservation due to the invariance of the PN Lagrangian under rotations and time translations [8]. This almost guarantees that the projection of the trajectory onto a 2D section of phase space will *not* be constrained to a 1D curve, so regular behavior could easily be misinterpreted as chaos (cf. [5,6]).

A more quantitative method for identifying and measuring chaos is to calculate the maximum Lyapunov exponent, defined as the divergence rate between initially nearby trajectories:

$$\gamma(t) \equiv \frac{1}{t} \ln\left(\frac{dX(t)}{dX(0)} \right). \tag{1}$$

Here the difference dX between two points in phase space is simply the Cartesian distance between the dimensionless 12-component coordinate vectors $[\vec{r}, \dot{\vec{r}}, \vec{S}_1, \vec{S}_2]$ and $[\vec{r}', \dot{\vec{r}}', \vec{S}_1', \vec{S}_2']$ of two nearby trajectories. In our numerical integrations, the initial separation is a small displacement in phase space with a random orientation and a magnitude of $dX(0) = 10^{-10}$. The two trajectories are then integrated forward in time, recording the separation $dX(t)$, from which γ is computed. In chaotic systems, the divergence will be exponential in time with a roughly constant (positive) exponent: $dX(t) \sim dX(0) \exp(\gamma t)$. To be precise, there are actually many different Lyapunov exponents, one for each dimension of phase space. The *maximum* Lyapunov exponent is automatically selected because, like a classical eigenvector problem, any vector (such as the random initial displacement vector) when multiplied repeatedly by the same matrix will grow fastest in the direction corresponding to the largest eigenvalue. Similarly, for a chaotic system, any random initial displacement in phase space is expected to grow as fast as the maximum Lyapunov exponent. However, for a regular system, the divergence generally grows linearly or at most as a power law in time. In that case, the Lyapunov exponent γ approaches zero for large t. We define the Lyapunov time $t_L \equiv 1/\gamma$ as the time scale on which nearby trajectories separate by a factor of e (the "*e*-folding time"). While it is difficult, on the basis of numerical integrations, to claim that a system is categorically nonchaotic on all time scales, we *can* make the more precise claim that on a particular time scale the

system shows no chaotic behavior; that is, we can set a lower limit on t_L. For the problem of coalescing compact binaries, the relevant time scale is the inspiral time t_{insp}, so if $t_{\text{insp}} \ll t_L$, chaos will not affect the dynamics.

To establish the validity of our numerical approach, we have reexamined the problem studied by Suzuki and Maeda [14], where both chaotic and regular trajectories have clearly been identified for supermaximally spinning test particles ($S_2 \gg m_2^2$; $m \gg \mu$) orbiting around a Schwarzschild black hole ($S_1 = 0$). While physically unrealistic, these conditions introduce no mathematical singularities into the equations of motion and are therefore fine examples for identifying chaotic or regular behavior in this dynamical system. Here we show numerical results for two different sets of initial conditions: both begin with $r/m = 4.5$, $\beta = 10^{-4}$, $S_1 = 0$, $S_2 = 1.4 \times 10^4 m_2^2$, and spin-orbit misalignment angle $\theta_2 = \pi/4$, but one trajectory has an initial Newtonian orbital angular momentum of $L_N/m = 1.485\mu$ while the other begins with $L_N/m = 1.53\mu$. In Fig. 1 we show the measured value of γ as a function of time (measured in orbital periods). The orbit with $L_N/m = 1.485\mu$ (a) is clearly chaotic with $\gamma \sim 0.1$ (corresponding to a divergence time scale of $t_L \sim 10$ orbital periods). The other trajectory (b) exhibits very different qualitative behavior, with no evidence for chaos even on the time scale of thousands of orbits. Our results for these and many other trajectories that we have computed agree well with Suzuki and Maeda's results, confirming that both chaotic and regular orbits exist for rapidly spinning test particles around a Schwarzschild black hole.

Another method for distinguishing between chaotic and quasiperiodic orbits is to look for certain qualitative features in the power spectrum of one of the dynamical variables [9,15]. For the compact binary problem, the obvious choice is to analyze the spectrum of the GW signal,
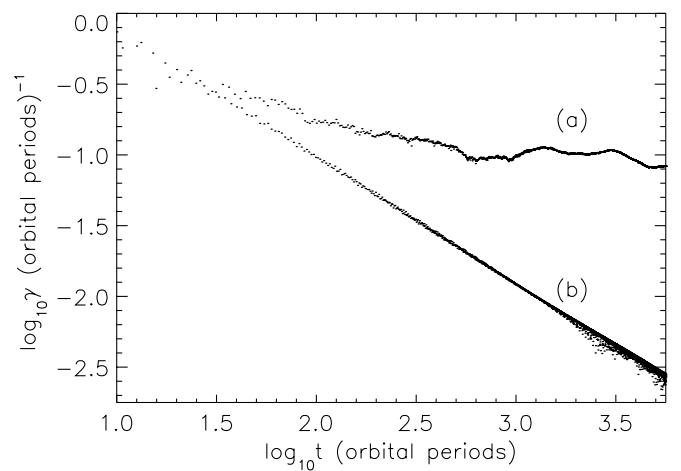

FIG. 1. Lyapunov exponent γ for test-particle orbits around a black hole. The orbits in case (a) are chaotic, with γ approaching a positive value corresponding to a divergence time of $t_L \sim 10$ orbital periods. The regular orbits in case (b) diverge linearly in time so that $\gamma(t) \to 0$.

defined as the squared amplitude of the Fourier transform of the GW strain $h(t)$. With RR turned off, the spectrum should exhibit sharp lines for quasiperiodic orbits, but broadband noise for chaotic orbits. Including only the leading quadrupole radiation terms, the components of the transverse-traceless GW tensor observed from the $\hat{z}$ direction are

$$h_+ = \frac{4\mu}{D}\left(v_x^2 - \frac{m}{r^3}x^2\right), \tag{2}$$

$$h_\times = \frac{4\mu}{D}\left(v_x v_y - \frac{m}{r^3}xy\right), \tag{3}$$

where D is the distance to the source and $v_i = \dot{x}_i$ [7,16]. Figure 2 shows the power spectra in $h_+(t)$ for the same two test-particle orbits as in Fig. 1. Both spectra show peaks around $f_{GW} \simeq 25$ Hz, the fundamental quadrupole frequency (twice the orbital frequency) for these initial conditions. As expected, the chaotic orbit (a) produces primarily broadband noise with few distinguishable features, whereas the spectrum for the quasiperiodic orbit (b) shows many sharp lines.

Having established the ability of our method to distinguish between regular and chaotic trajectories described by the PN equations of motion, we now apply the same techniques to the astrophysically relevant systems expected to be detectable by ground-based laser interferometers. Here we will show results for an illustrative case of two maximally spinning $10M_\odot$ black holes ($S_i = m_i^2$) in an initially circular orbit with spin-orbit misalignment angles of $\theta_1 = 38°$ and $\theta_2 = 70°$. To measure the Lyapunov exponent at different points during the final inspiral, four different trajectories were integrated, corresponding to GW frequencies of 10, 40, 100, and 400 Hz, emitted at orbital separations $r/m \simeq 50$, 20, 10, and 5, respectively [17]. For each separation, we then integrate the PN equations of

motion (with RR turned off) over a period much longer than the inspiral time. If no exponential divergence is observed, we can safely conclude that the system is, for all practical purposes, not chaotic.

The measured values for $\gamma(t)$ are plotted in Fig. 3 for each of the selected stages of the inspiral. For any power-law divergence in phase space with $dX(t) \sim t^\alpha$, on a log-log plot of γ versus time the slope is $d\ln\gamma/d\ln t = 1/\ln t - 1$, so that for large times the curve should be linear with slope -1 [as we see in Fig. 1(b)]. All plots in Fig. 3 clearly show this behavior, characteristic of regular, nonchaotic orbits. Also shown for comparison in Fig. 3 are the inspiral times corresponding to each separation. In all four cases, the lower limit on t_L far exceeds t_{insp}.

Just as in the test particle example presented above, we also calculate the gravitational wave power spectrum for this black hole binary. Here the results are even more striking: Fig. 4 shows the $h_+(t)$ power spectrum at the point in the inspiral where the GW frequency is 100 Hz. The spectrum has a few very sharp lines with no evidence for broadband noise. The strongest features correspond to the fundamental GW quadrupole and spin-orbit precessional frequencies (100 and 7 Hz, respectively) and their harmonics. The spectra from the other points in the inspiral show the same qualitative features, all indicative of quasiperiodic motion.

In addition to this prototypical binary black hole system, we have investigated the behavior of a large number of other systems at different stages throughout the inspiral. Varying the binary mass ratio, spin magnitudes (always with $S_i \leq m_i^2$), misalignment angles, eccentricity, and initial separation over wide ranges, we consistently find the same regular, nonchaotic behavior for all trajectories. In particular, we have calculated orbits for the same high-eccentricity systems considered by Levin in Ref. [5] and again measure only linear divergence of nearby initial
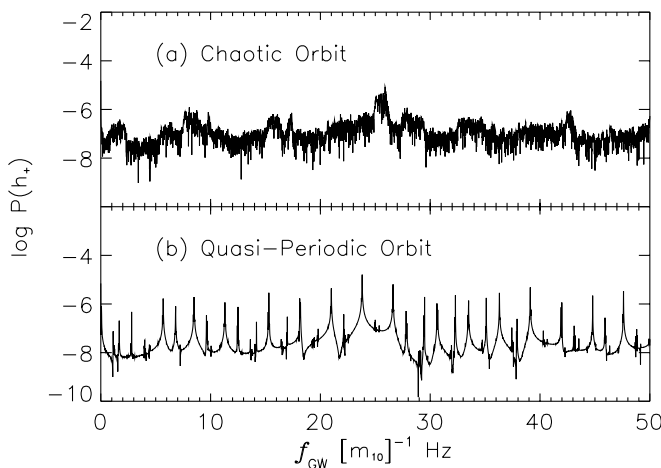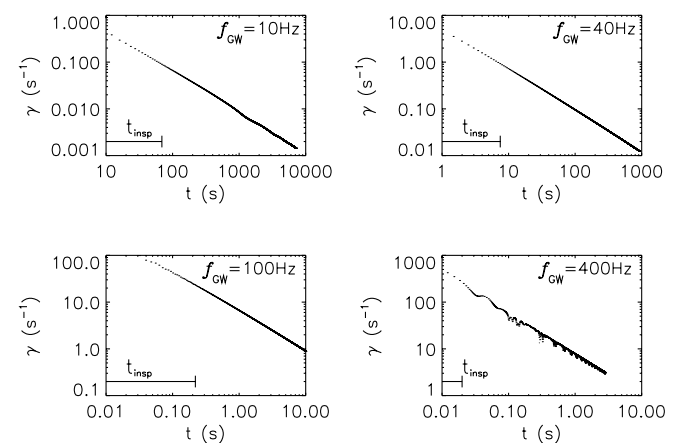

FIG. 2. Power spectra of the GW signal $h_+(t)$ for the same two cases as in Fig. 1. The chaotic system in (a) produces broadband noise while the quasiperiodic orbit (b) exhibits sharp spectral lines. The GW frequency is given in units of m_{10}^{-1} Hz, where $m_{10} = m/10M_\odot$.

FIG. 3. Lyapunov exponent $\gamma(t)$ for different stages in the inspiral of two maximally spinning $10M_\odot$ black holes: $f_{GW} = 10$ Hz, $r/m = 47.25$, $t_{insp} = 69$ s; $f_{GW} = 40$ Hz, $r/m = 18.75$, $t_{insp} = 7.5$ s; $f_{GW} = 100$ Hz, $r/m = 9.2$, $t_{insp} = 0.2$ s; $f_{GW} = 400$ Hz, $r/m = 4.0$, $t_{insp} = 0.01$ s. No evidence for chaos is seen, with $t_L = 1/\gamma \gg t_{insp}$ in all cases.
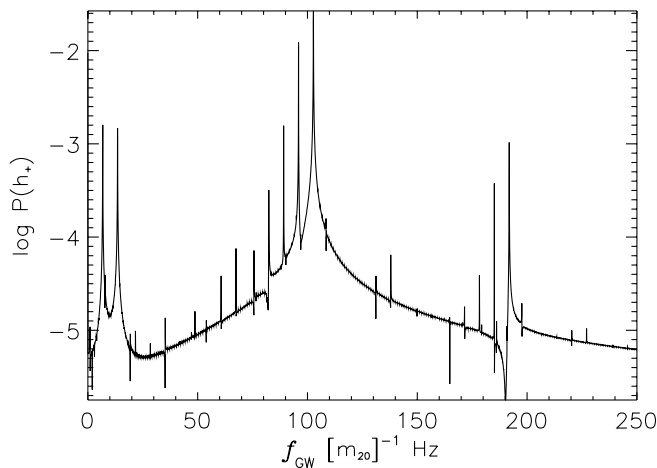
FIG. 4. Power spectrum of the GW signal $h_+(t)$ calculated from the initial conditions of Fig. 3 at the stage in the inspiral where $f_{GW} = 100$ Hz. The frequency is in units of m_{20}^{-1} Hz, where $m_{20} = m/20M_\odot$. The sharp lines in the spectrum confirm that the orbit is regular.

conditions, finding $t_{insp} \ll t_L$ [18]. We have also looked at many binary systems in which either one or both objects are solar-mass neutron stars. Because of their smaller mass (and thus slower radiation loss), these systems can spend significantly longer times in the inspiral band, completing tens of thousands of orbits before merger. Yet, even on the longest relevant time scales ($t_{insp} \gtrsim 10^4$ s), we again find no chaotic behavior.

Recent work in binary star evolution [19] suggests that systems with large spin misalignment angles are likely to be astrophysically relevant sources, giving rise to complicated nonlinear SO and SS interactions. It is possible that there are undiscovered narrow regions in phase space where specific resonant conditions could give rise to chaotic behavior, yet even if a binary system passes through them during inspiral, the time spent in these resonant bands will most likely be much shorter than the Lyapunov time. Even though the Lyapunov exponent approaches zero for all the systems we have considered, their orbits can still appear quite irregular, especially when both objects are spinning rapidly [5]. As mentioned above, this can lead to the spreading of the surface of section away from a 1D curve, but in dynamical systems with many degrees of freedom, this spreading alone does not imply the presence of chaos. Nevertheless, the detection of GW signals from binaries with rapidly spinning components may be very challenging. Systems with similar initial conditions still may produce waveforms that look quite different even without exponential divergence. Orbital precession will add many complicated features to the basic inspiral waveforms. The current template database will most likely need to be extended (perhaps by orders of magnitude) to include at least a portion of parameter space where the signals are significantly modified by spin effects [20]. Furthermore, for the late stages of inspiral, the

2.5PN expansion becomes invalid and one should include higher order PN terms (or even perform calculations in full general relativity [21]). While these terms introduce additional features in the dynamics, at this late stage the orbit is certainly decaying too rapidly for the final GW signal to be affected by formal chaotic behavior.

*Electronic address: schnittm@mit.edu
†Electronic address: rasio@mit.edu

[1] K. S. Thorne, in *300 Years of Gravitation,* edited by S. W. Hawking and W. Israel (Cambridge University Press, New York, 1989); B. F. Schutz, Classical Quantum Gravity **6**, 1761 (1989).
[2] C. Cutler *et al.,* Phys. Rev. Lett. **70**, 2984 (1993).
[3] B. J. Owen and B. S. Sathyaprakash, Phys. Rev. D **60**, 022002 (1999).
[4] B. Allen *et al.,* Phys. Rev. Lett. **83**, 1498 (1999).
[5] J. Levin, Phys. Rev. Lett. **84**, 3515 (2000).
[6] J. Levin, gr-qc/0010100.
[7] L. E. Kidder, Phys. Rev. D **52**, 821 (1995).
[8] L. E. Kidder, C. M. Will, and A. G. Wiseman, Phys. Rev. D **47**, 3281 (1993).
[9] G. Sussman and J. Wisdom, Science **241**, 433 (1988).
[10] N. J. Cornish, Phys. Rev. Lett. **85**, 3980 (2000).
[11] C. D. Murray and S. F. Dermott, *Solar System Dynamics* (Cambridge University Press, Cambridge, 1999).
[12] J. Wisdom (private communication).
[13] We do not consider the spin momenta as dimensions in phase space since they play no role in the equations of motion. The precession equations in [7] independently give the instantaneous spin momenta in terms of other phase-space variables.
[14] S. Suzuki and K. I. Maeda, Phys. Rev. D **55**, 4848 (1997).
[15] Note, however, that the use of power spectra is a more qualitative technique for identifying chaos, which can sometimes be misleading; see G. Sussman and J. Wisdom, MIT AI Laboratory Memo 1359 (1992).
[16] C. W. Misner, K. S. Thorne, and J. A. Wheeler, *Gravitation* (W. H. Freeman and Company, New York, 1973).
[17] These four different trajectories are actually all computed from the same initial conditions at $r/m = 47.25$, turning on RR to evolve the system from one stage to the next.
[18] Since RR tends to circularize orbits, the eccentricity of any astrophysically relevant systems should actually be extremely small by the time they evolve to $f_{GW} \sim 10$ Hz; see K. Belczynski, V. Kalogera, and T. Bulik, Astrophys. J. (to be published).
[19] V. Kalogera, Astrophys. J. **541**, 319 (2000).
[20] T. A. Apostolatos, C. Cutler, G. J. Sussman, and K. S. Thorne, Phys. Rev. D **49**, 6274 (1994); T. A. Apostolatos, Phys. Rev. D **52**, 605 (1995).
[21] A. Buonanno and T. Damour, Phys. Rev. D **59**, 084006 (1999).